Final Version June 25, 2020
Typeset using LaTeX default style in AASTeX63

An Overview of Low-Mass Stellar Evolution

Scott Tompkins[1]

[1]School of Earth and Space Exploration, Arizona State University, Tempe, AZ 85287-1404

Abstract

I use the 1-D stellar evolution code MESA to run a series of stellar models at and below 1.1 solar masses, examining the effects of mass and metallicity on stellar evolution. In doing so, I sort the models in a grid of 77, running 7 different metallicity values for each mass. I examine end stages, main sequence lifetime dependencies, and other observable characteristics. Primarily, I find that end stage as a white dwarf depends only on mass and not on metallicity. For all stars above 0.5 $M_\odot$, helium burning begins and this indicates that the model will finish as a carbon white dwarf. For models at or below this mass, no helium burning occurs that will result in helium white dwarf formation. I find that, unsurprisingly, there has not been enough time for any helium white dwarf to form from a single star as the minimum lifetime of a star to form one is found to be on the order of 80 *Gyr*, nearly six times the current age of the universe. I also demonstrate key nontrivial differences in evolution between stars at different masses involving main sequence convection. Next, I demonstrate post-main sequence evolutionary milestones as shown in select models which had helium burning and display these traits clearly. Finally, I examine metallicity dependence and lifetime, demonstrating almost no difference in lifetime for any Z values other than solar metallicity. I also find almost no difference in evolution between big bang metallicity, 10^{-10} $Z_\odot$ and zero metallicity at masses of 0.6 $M_\odot$ and above.

Keywords: Low-Metallicity, White Dwarfs, Low-Mass Stars

1. INTRODUCTION

In this paper, using the MESA stellar evolution code, I analyze the effect of mass and metallicity on stellar evolution at and below 1.1 solar masses, with each mass running metallicity values between solar metallicity, $Z_\odot$ and zero metallicity. The purpose of this research was to see if at any point metallicity would impact the end stage of the star's evolution and whether it would end as a carbon-oxygen white dwarf or as a helium white dwarf. This work is a follow-up to my first paper on stellar evolution in my thesis with Barrett Honors College in which I attempted to replicate and explain a result in *Windhorst et al. (2018)*, in which the model at M=1.0 $M_\odot$ and Z=0 did not ignite helium, and thus may turn directly into a helium white dwarf, but a model at M=1.0 $M_\odot$ and Z=10^{-8} $Z_\odot$ did ignite helium. Initially, I theorized that there was a critical Z value between these two bounds where above this value, helium would ignite, and below this value, it would not. I tried and failed to reproduce this result in both of my attempts. The zero metallicity solar mass star did ignite helium. In this case, the model at M=1.0 $M_\odot$ and Z=0 completed its evolution and ended as carbon-oxygen white dwarf.

After running and analyzing lower mass models, I found no case in which metallicity alone affected the outcome of stellar evolution. With a mass spacing of 0.1 $M_\odot$, all models at or above 0.6 $M_\odot$ ended with the formation of a C-O white dwarf and below this mass, helium white dwarfs formed, with no dependence on metallicity. Had I been able to produce a helium white dwarf from a 0.9 $M_\odot$ model or higher due to metallicity dependence, this would have indicated that helium white dwarfs could have formed from a single star within the current age of the universe. However, my results agree with those of *Zenati et al. (2018)*, where the authors used a different stellar evolution modeling code to

satompki@asu.edu

show that the minimum mass of a present day white dwarf formed from a single star is in the range of 0.50-0.52 $M_\odot$. Their models were stars in the mass range from 1.01-0.84 $M_\odot$ where Z values range between 1.5 $Z_\odot$ and 0.1 $Z_\odot$. The majority of my models were run below this Z range. However, some of the models at 0.8 $M_\odot$ managed to run until a degenerate C-O core formed with a mass of 0.55 $M_\odot$ and an age of 13.2 *Gyr*. Given that these models were run at much lower Z values, and that in my previous work I found that Z value of 0.1 $Z_\odot$ still significantly affected stellar lifetime, my results are comparable to the results of *Zenati et al. (2018)*.

I also examine post-main sequence evolution of the models which managed to run past the main sequence, specifically looking at the evolution onto the AGB and the presence of thermal pulses. As originally discussed in *Schwarzschild and Harm, (1965)*, stars at 1.0 $M_\odot$ undergo a series of thermal instabilities where helium burns explosively on the surface of a partially degenerate core. These pulses occur as conditions become sufficient for small amounts of helium to burn explosively, and the pulses move inwards burning helium, but they do not consume all of the helium. These pulses, as described in *Pols et al. (2001)*, have important consequences for the nucleosynthesis of heavier elements and their transport to the surface through dredge up events.

Finally, I examine the effect of metallicity on main sequence lifetime which is briefly discussed in *Vassiliadis and Wood (1993)* for stars at 1.0 $M_\odot$. Almost all of my models are at much lower Z values than the models run here, but the results of these models agree with the main sequence lifetimes of their lowest Z model. In my MESA model running a Z value of Z=10^{-4} $Z_\odot$ and a mass of 1.0 $M_\odot$ the end of the main sequence begins at an age of 5.74 *Gyr*. This agrees remarkably well with the results of *Vassiliadis and Wood (1993)*, which had a model at 1.0 $M_\odot$ and Z=0.001 which had the same main sequence lifetime. As a part of my results, I show that metallicity has almost no effect on lifetime for the values chosen, and all models which ran to completion except those at solar metallicity have nearly identical main sequence lifetimes. In my previous work with MESA, I ran a model with identical mass and metallicity to the model in their paper and the main sequence lifetime was still the same. This shows how little of an effect metallicity has on main sequence lifetime even at 5% of solar metallcity.

2. MASS, METALLICITY, AND THE END STAGE OF STELLAR EVOLUTION

As the original purpose of my investigation, I find that metallicity has no effect on whether a helium or carbon-oxygen white dwarf forms. WD formation and composition appears to only depend on mass, with all models at or below 0.5 $M_\odot$ forming helium white dwarfs, and all models above this mass forming carbon-oxygen white dwarfs. The result is captured in the following figure.

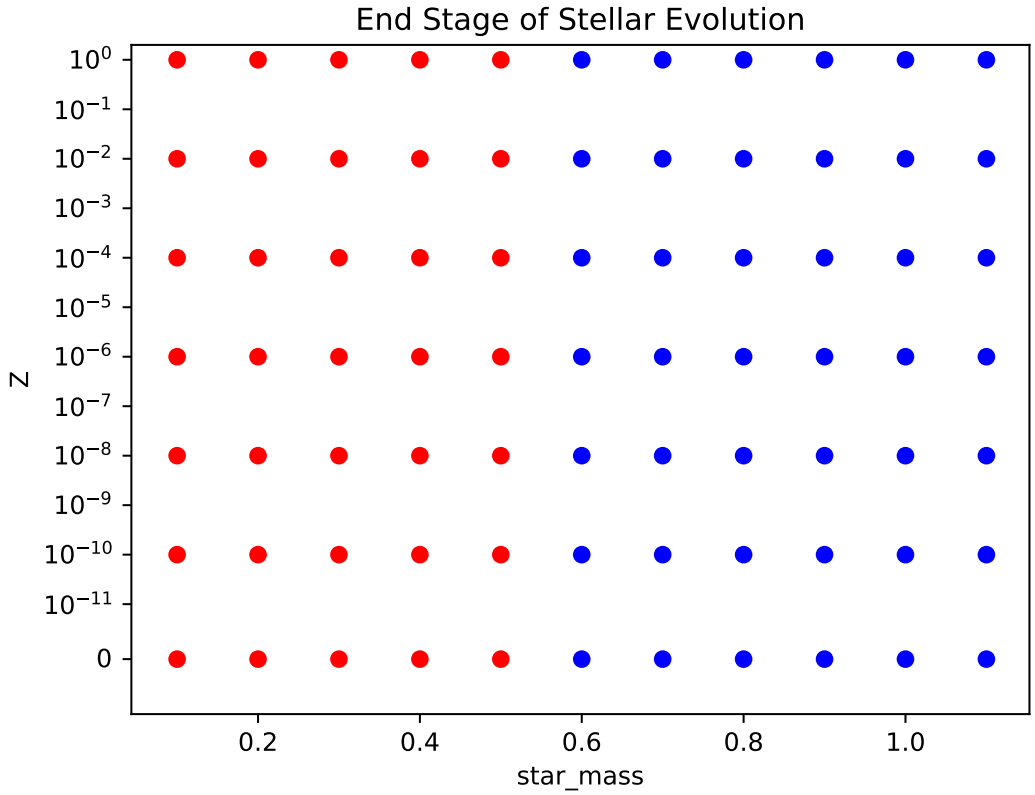

Figure 1. A scatter plot showing the end stages of stellar evolution for each model. Red points represent helium white dwarfs and blue points represent carbon white dwarfs. Metallicity is plotted as $Z_{\odot}$.

This result does not match what I hypothesized to be the case, in which metallicity would at some point have an impact on the end stage of stellar evolution. The hypothesis came from my previous work in MESA, in which I tried to replicate a previous result in *Windhorst et al. (2018),* in which a zero metallicity solar mass star did not ignite helium. In concluding this previous project and finding helium burning in every case, I began to think that metallicity can have an impact on the end stages of low mass stars at lower masses. I thought this would be the case due to differences in core temperatures reached I believed to exist, as core temperature is the primary factor behind driving energy generation in stars. However, the data does not indicate this. For models of the same mass, central temperatures were taken at equivalent points during stellar evolution, chosen to be when the core hydrogen fraction had reached half of its original value. The models at zero metallicity were consistent in having a higher core temperature but the difference is small. Central temperature at this evolutionary milestone did have a stronger correlation with mass, as the central temperatures between the lowest and highest mass models that ran successfully at 0.2 and 1.1 solar masses had a core temperature difference of around a factor of 2. The data was taken from the live output files provided by MESA, and is tabulated below. The accompanying figure compares core temperature at zero and solar metallicity at 0.6 $M_{\odot}$ showing that when age is normalized to one for comparison, the zero metallicity model has consistently higher core temperatures until nuclear burning stops.

It should be noted that there were a few models that when looking at the live output appeared to violate this, but all of these cases lie at 0.6 $M_{\odot}$ and above had began the helium flash. Thus had they been allowed to finish running, then they would have finished as a carbon white dwarf. These models had the maximum allowed runtime of 96 hours, and it is difficult to determine what would have allowed them to finish. No helium flash occurs at or below half a solar mass, and some of these models finished their evolution and produced helium white dwarfs, while others had difficulty pushing through the main sequence while running. However, due to their consistently lower central temperatures than the confirmed helium white dwarfs at 0.5 $M_{\odot}$, it is safe to conclude that they would have ended as helium white dwarfs.

Mass $M_\odot$	T(K×10^6) Z = 0	T(K×10^6) Z = $Z_\odot$
0.2	8.96	8.75
0.3	9.43	8.87
0.4	9.41	8.62
0.5	10.5	9.70
$M_\odot$ 0.6	11.7	10.4
0.7	13.7	11.5
0.8	14.4	13.0
0.9	16.1	13.5
1.0	17.7	15.4
1.1	18.7	16.0

Table 1. Core temperature at half hydrogen depletion for models at $Z_\odot$ and Z=0. The zero metallicity values are higher at all times during the main sequence.

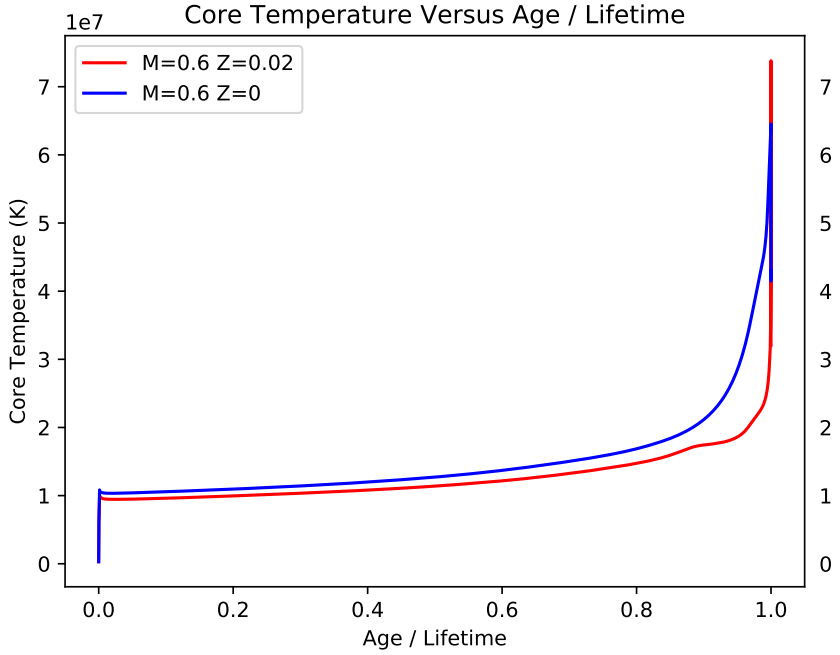

Figure 2. Core temperature versus age *(normalized to one)* for a select mass where models ran well. Core temperature at *Z=0* is consistently higher, but the difference is small.

This behavior is seen at every mass comparing solar and zero metallicity, which further backs up the idea that a non-helium burning sun at zero metallicity will simply not happen. If anything, the consistently higher core temperatures will make it easier for low metallicity models to ignite helium and end as carbon white dwarfs. Thus the data suggests dependence of end stage on metallicity will be the reverse of what was initially proposed if it is ever found in future *MESA* models, with higher Z increasing the chances of stars on the mass border between 0.5 and 0.6 $M_\odot$ being helium white dwarfs. For the purposes of this paper, however, no correlation between metallicity and end stage can be established and this must be done in future work on a narrower range of masses. One can compare the two models on the boundary with the closest core temperatures. The 0.5 and 0.6 $M_\odot$ models at zero and solar metallicity, respectively. The maximum core temperature reached differs by nearly 10 million K as a result of the helium flash occurring in one in one model and not the other. The core temperature of the 0.5 $M_\odot$ model reaches a maximum and cools exponentially as it becomes a white dwarf, while the 0.6 $M_\odot$ model never made it to the white dwarf stage. These aspects are shown in the figure below.

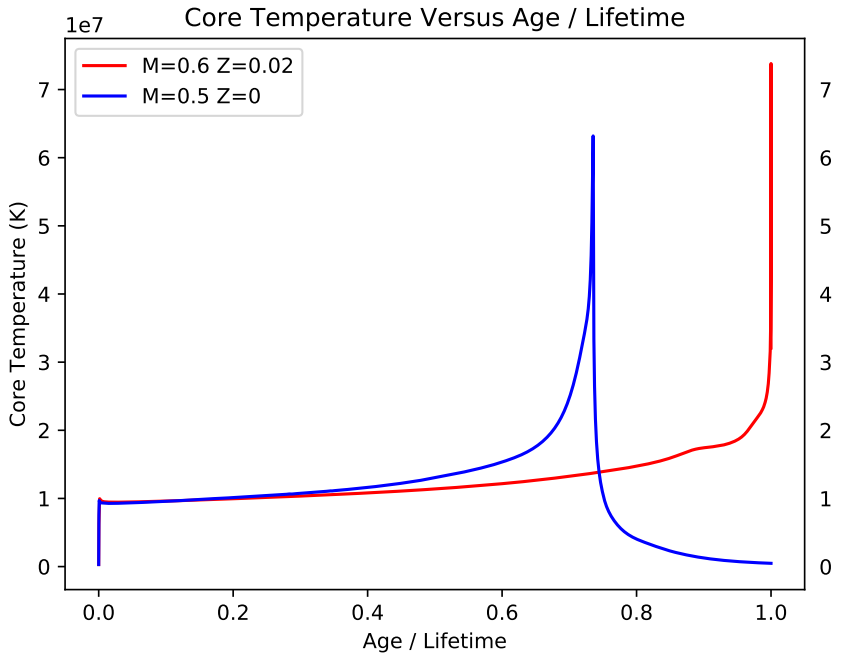

Figure 3. Core temperature versus age *(normalized to one)* for two different masses across the helium burning boundary which had the most similar core temperatures. The model at 0.5 $M_\odot$ reaches a maximum of 6.3×10^7 K and the model at 0.6 $M_\odot$ reaches a maximum of 6.4×10^7 K. The difference is sufficient to allow helium burning in one case and prevent it in the other.

The changes caused by this difference in maximum core temperature produce the dramatically different results shown in the following temperature-density profiles. The 0.5 $M_\odot$ model never reaches a temperature sufficient to burn helium, while the 0.6 $M_\odot$ easily reaches beyond this temperature. Equation of state boundaries are shown and labeled, which show if the star has sufficient conditions to burn helium.

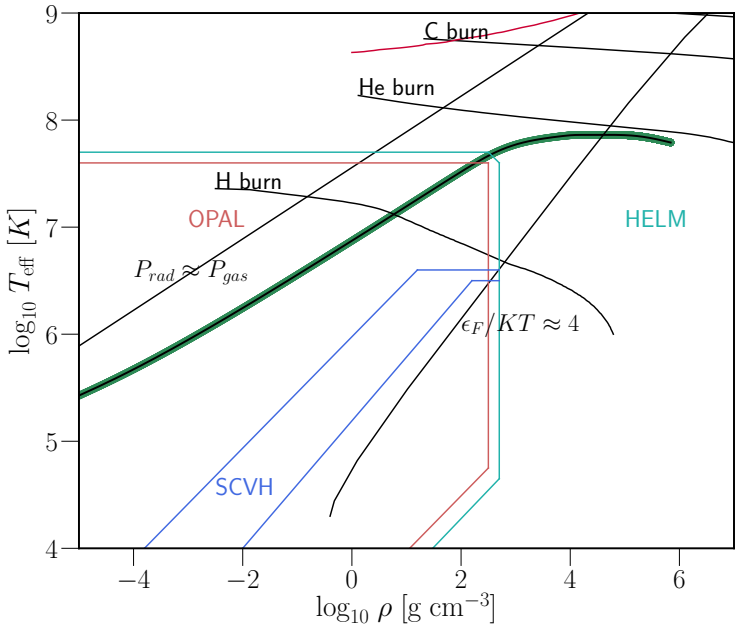

Figure 4. A temperature-density profile taken when the 0.5 $M_\odot$ and zero metallicity reaches maximum core temperature. Helium burning conditions are never met and hence a helium white dwarf is formed as hydrogen shell burning throws off the outer layers of the star.

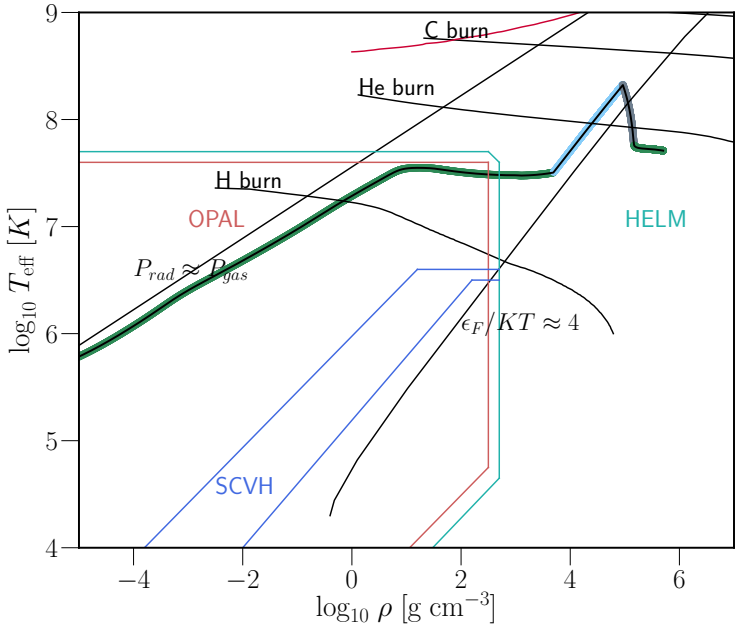

Figure 5. A temperature-density profile taken when the 0.6 $M_\odot$ model reaches maximum core temperature. The conditions are more than sufficient to burn helium, and the helium flash is occurring as this profile is taken. This model will go on to form a carbon white dwarf.

3. SHOWING THE VALIDITY OF THE ZERO METALLICITY APPROXIMATION FOR THE FIRST STARS

Here I demonstrate the validity of the zero metallicity assumption for the first stars in this mass range by comparing the big bang abundance of 10^{-10} $Z_{\odot}$ and zero metallicity. There are almost no differences in the HR diagram evolution of these stars at the same mass, with many of the figures being completely overlaid on each other. This is due to the fact that for all but the 1 and 1.1 $M_{\odot}$ models, heavy elements play almost no role in energy generation and proton-proton chain burning, which does not require any heavy elements and is the only significant source of energy in all models below 1.0 $M_{\odot}$ until post-main sequence burning. For the two highest mass models, the absence of catalysts for CNO burning does have an effect on evolution which is identical for both masses and Z values. I discovered this effect in a previous work, and it is a result of the model very slowly producing CNO elements on the main sequence. During the transition onto the RGB, a critical threshold is reached and there is enough of these elements to let CNO burning happen, which briefly causes the core to be convective and provides a new source of energy which increases the luminosity and surface temperature of the star, which is seen as a loop on the HR diagram.

There are slight differences in evolution for models at 0.3 and 0.4 $M_{\odot}$ but the HR diagrams show the main sequence. The differences arise after the main sequence and since there were problems in the models at this mass range in which energy generation spikes occurred randomly with no apparent cause. What is shown as the looping behavior on the HR diagram happens for all models in this mass range with no apparent dependence on composition. There is one notable exception to this case, which occurred at 0.5 $M_{\odot}$. The zero metallicity model behaved normally and even formed a helium white dwarf, which is seen forming and cooling in the HR diagram, while the 10^{-10} $Z_{\odot}$ appeared to completely fail. This model reached a luminosity in excess of 10^4 $L_{\odot}$ and a surface temperature on the order of 10^5 K, and this is obviously a nonphysical scenario where the model had to be discarded. The same random spikes in energy generation occur in this model, but do not disappear and lead to what appears to be a P-P driven helium flash, which causes the nonphysical increases in effective temperature and luminosity. This HR diagram is shown in the appendix. Similar behavior was seen in the 0.3 $M_{\odot}$ models at $Z_{\odot}$ and 10^{-10} $Z_{\odot}$ as well but did not have severe consequences but does account for their differences in the following figures.

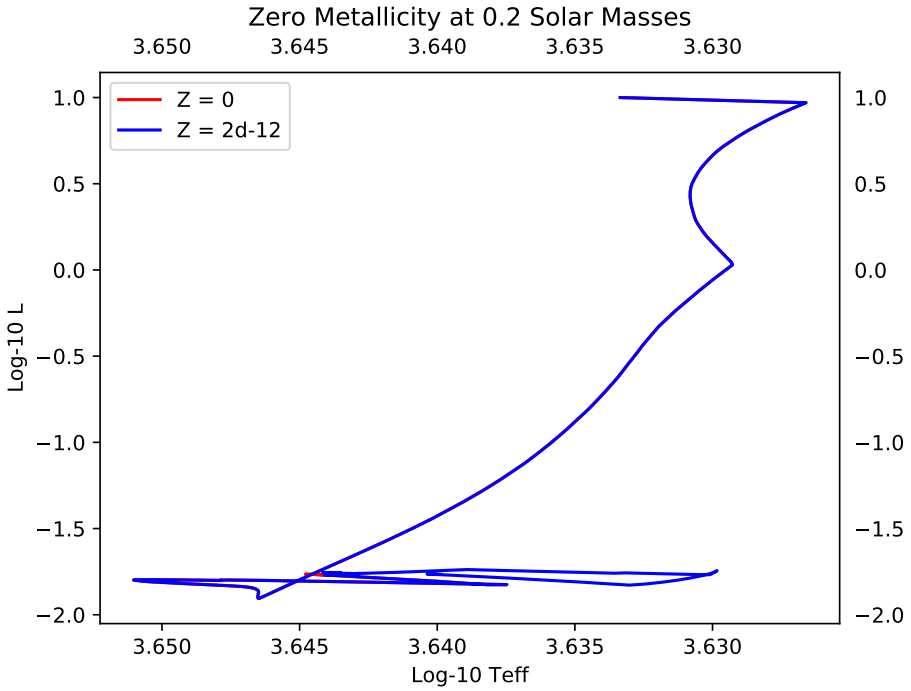

Figure 6. Comparing the HR diagram evolution at 0.2 $M_{\odot}$ where the models are nearly identical. Neither of these models ever reach core hydrogen depletion, but these two reached the same fraction out to two significant figures.

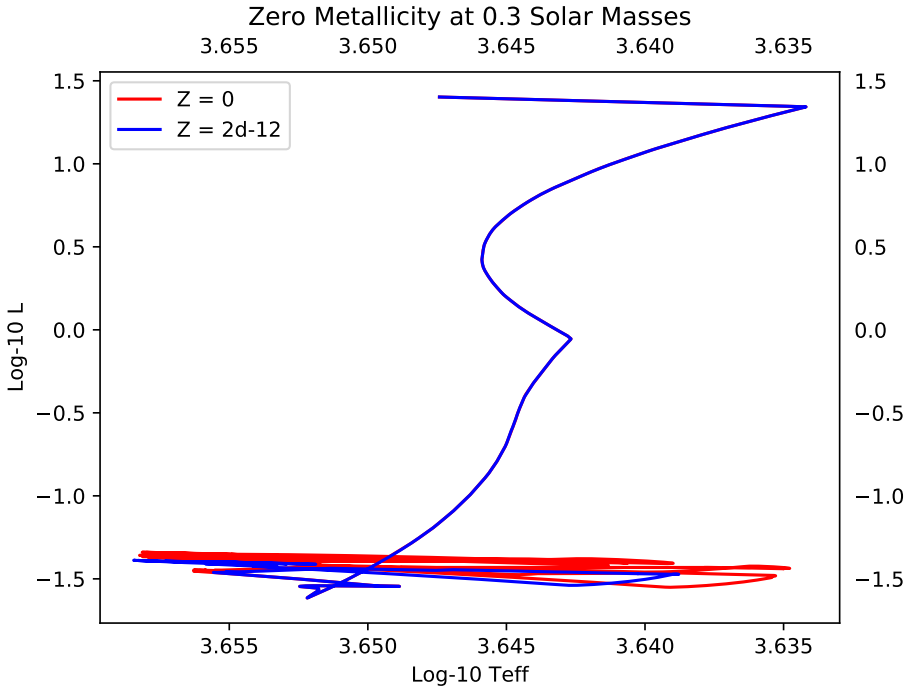

Figure 7. Comparing the HR diagram evolution at 0.3 $M_{\odot}$. Slight differences during the main sequence occur. Neither of these models ever reach core hydrogen depletion.

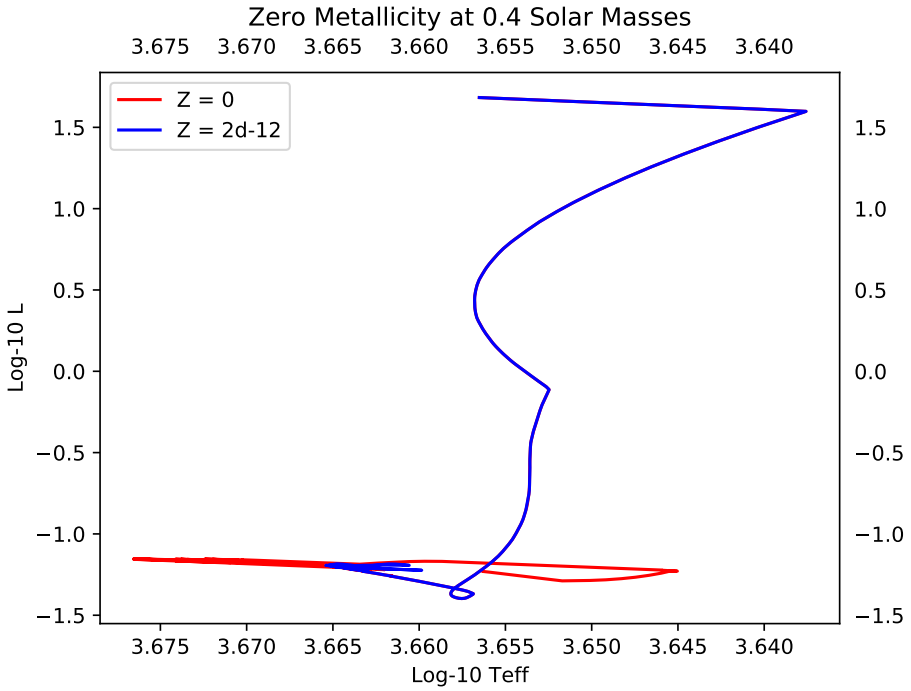

Figure 8. Comparing the HR diagram evolution at 0.4 $M_\odot$. Similar to the previous two figures, core hydrogen depletion never occurs.

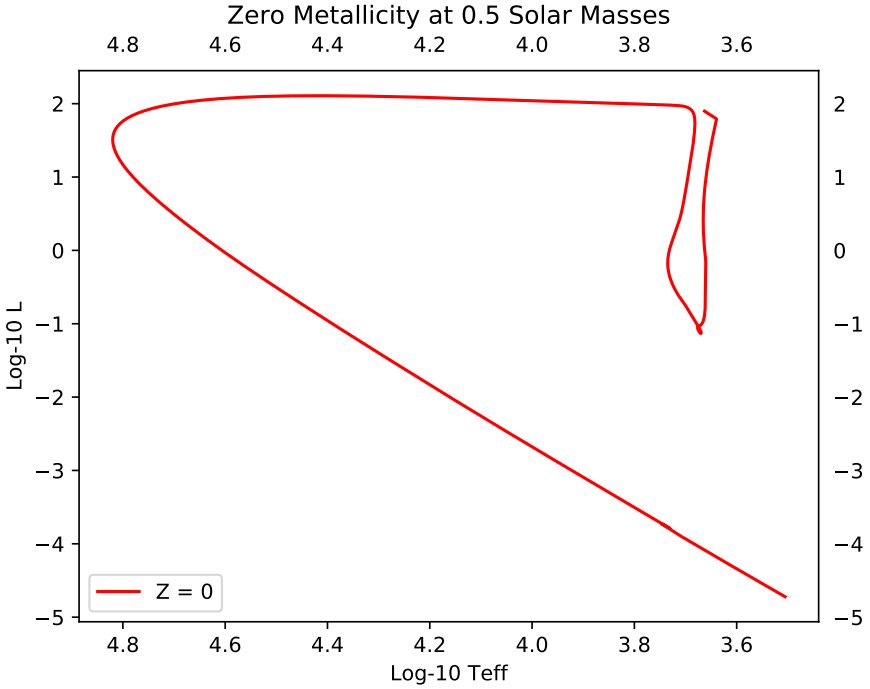

Figure 9. Comparing the HR diagram evolution at 0.5 $M_\odot$. The 10^{-10} $Z_\odot$ model is not included due to issues, but it is shown in the appendix. A helium white dwarf forms and is shown cooling.

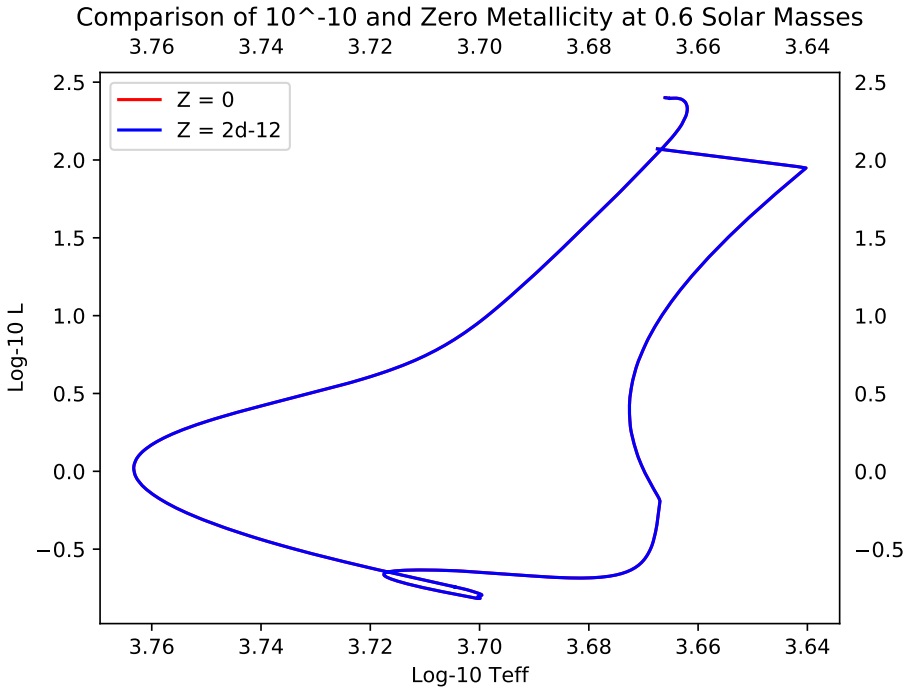

Figure 10. Comparing the HR diagram evolution at 0.6 $M_\odot$ with no visible differences. The figure looks exactly the same for all subsequent masses, with the two HR diagrams being indistinguishable.

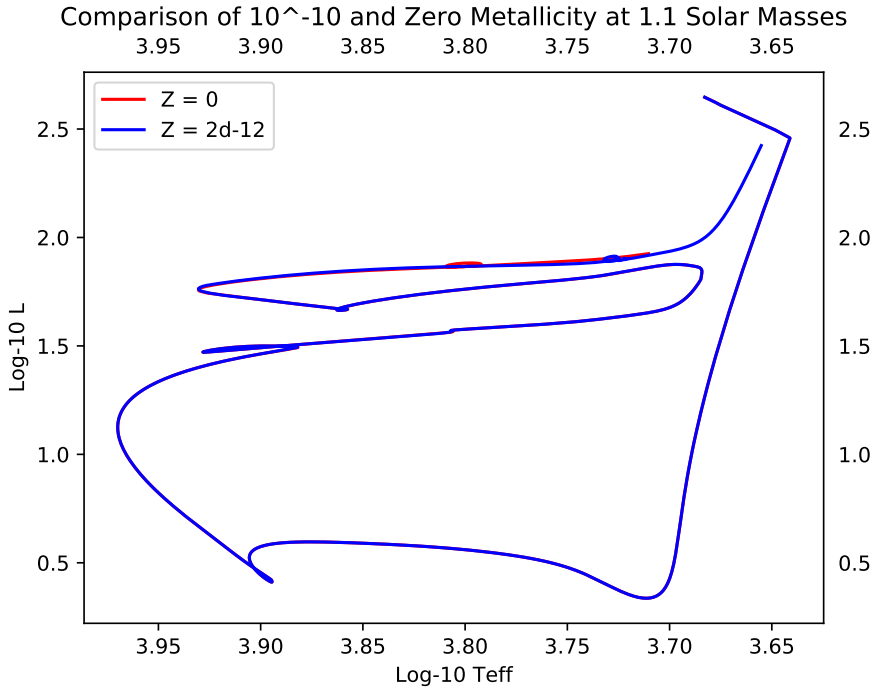

Figure 11. Comparing the HR diagram evolution at 1.1 $M_\odot$. Note the small loop occurring as the star evolves onto the RGB, discussed above. A classical blue loop is visible as well.

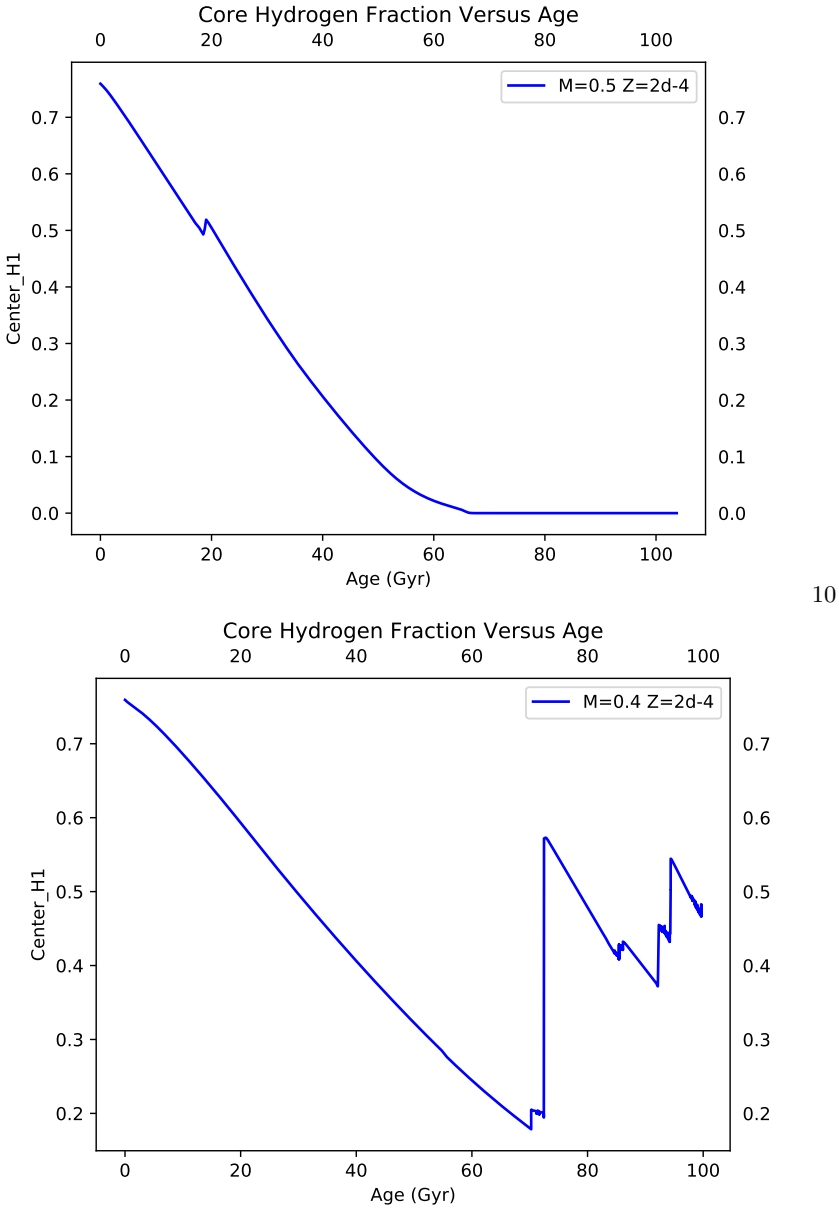

Figure 12. Core hydrogen fraction as a function of age for two models at 0.5 $M_\odot$ and 0.4 $M_\odot$ with the same metallicity of 10^{-2} $Z_\odot$, showing the two different types of behavior. The first model shows core hydrogen decreasing consistently throughout the main sequence while the second shows several instances of core hydrogen being replenished.

4. DISCUSSION OF MASS AND STELLAR EVOLUTION

Here I discuss some of the evolutionary differences between models at different masses. The primary nontrivial difference in evolution I find occurs on the main sequence at the mass boundary of 0.4 $M_\odot$ in which core hydrogen fraction does not continuously drop as the model ages. I found these differences in attempting to classify an end to the main sequence by looking at core hydrogen fraction as a function of age. In models above 0.4 $M_\odot$ the core hydrogen fraction decreases consistently with age allowing an easy comparison point for the models as this fraction reaches a critical value. However, in models below this mass, there are several instances in which the core hydrogen fraction increases on the main sequence. I display these results in comparing models at the same metallicity above and below this mass threshold. This occurs because instances of convection within the area around the core are able to replenish the core hydrogen from regions where burning was not occurring, or is happening at a much lower rate.

This is demonstrated in the following Kippenhahn diagrams showing the burning and convective regions of the star at as a function of age. There are three instances in the 0.4 $M_\odot$ model has core hydrogen replenished and this is visible as three brief convective episodes happening past an age of 60 *Gyr*. For the model at 0.5 $M_\odot$, no convection occurs and as shown in the core hydrogen plot, no new material for nuclear burning ever enters the core and hydrogen fraction only decreases.

The small bump seen in the top diagram of figure 12 at 20 *Gyr* also shows up as small convection period at the same time in figure 13. It is linked to one of the brief spikes in excess energy generation right at the core. This behavior was discussed earlier, and since it led to the failure of three models, it is safe to dismiss these.

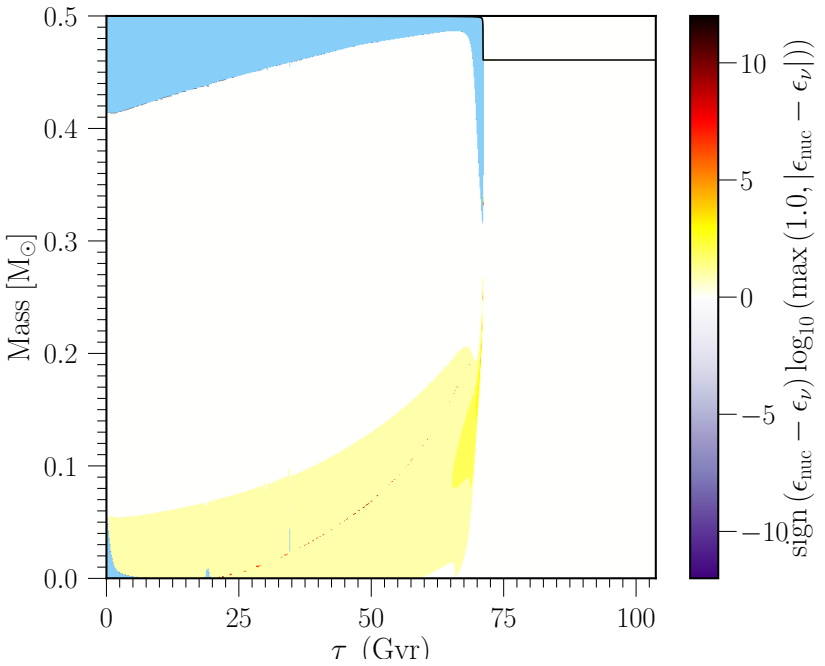

Figure 13. The Kippenhahn diagram for the model at 0.5 $M_\odot$. No convection occurs which is able to bring hydrogen back into the core, and thus core hydrogen fraction continuously decreases. Burning regions are shown in the orange heat-map.

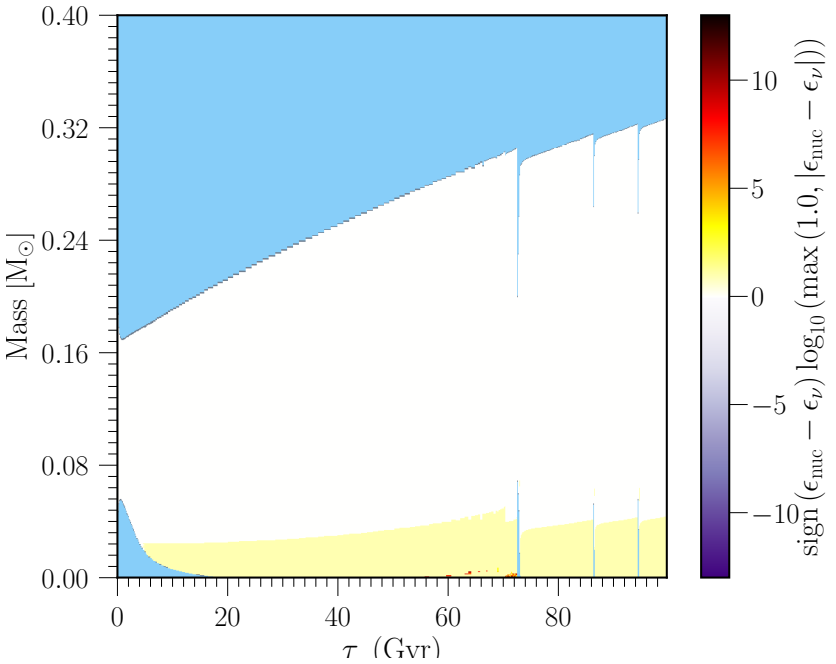

Figure 14. The Kippenhahn diagram for the model showing hydrogen replenishment. Convective regions are shown in light blue, and appear in the core during main sequence burning on the bottom right as small spikes.

There are other mass dependent features worth discussing here including for the single model at 0.1 $M_\odot$ and the higher mass models which managed to burn helium. In the 0.1 $M_\odot$ model, the star is fully convective, a feature unique to this mass range as shown by the data. While other masses had brief convective episodes that were able to resupply the core with hydrogen to burn, this model had continuous convection and was able to burn its entire mass into helium and become degenerate. The helium core mass and stellar mass had converged to the same value within seven significant figures when the model was terminated. The full convection manages to bring the helium to the surface as well. Thus this process, if any stars of this mass had evolved to this point, would be observable. The Kippehahn diagram is shown for this model below, which was running at 10^{-2} $Z_\odot$.

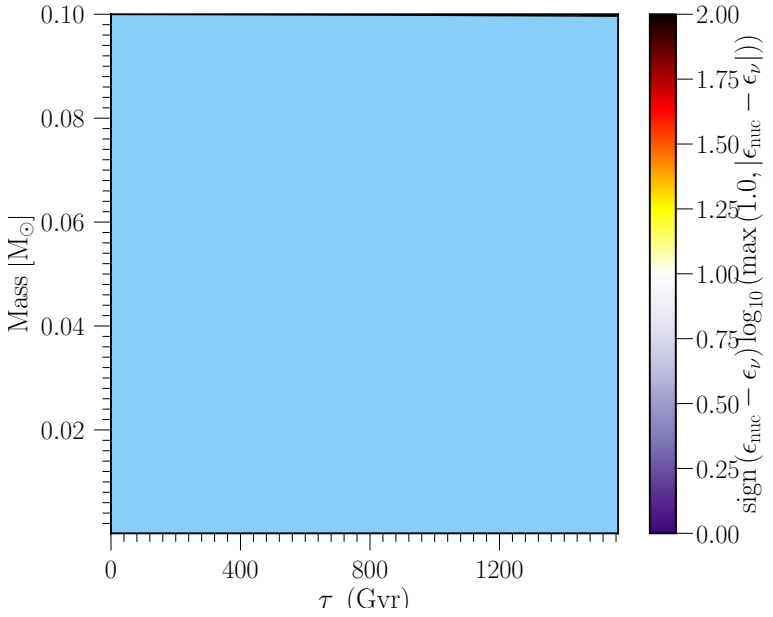

Figure 15. The Kippenhahn diagram for the model at 0.1 $M_\odot$. The model is fully convective at all times as shown in blue, and this is responsible for it turning nearly its entire mass into helium and its incredibly long lifetime.

While fully convective, the 0.1 $M_\odot$ model does not display this core replenishment and instead follows the trend of continuously decreasing core hydrogen fraction as new hydrogen is continuously brought into the core rather than in brief episodes.

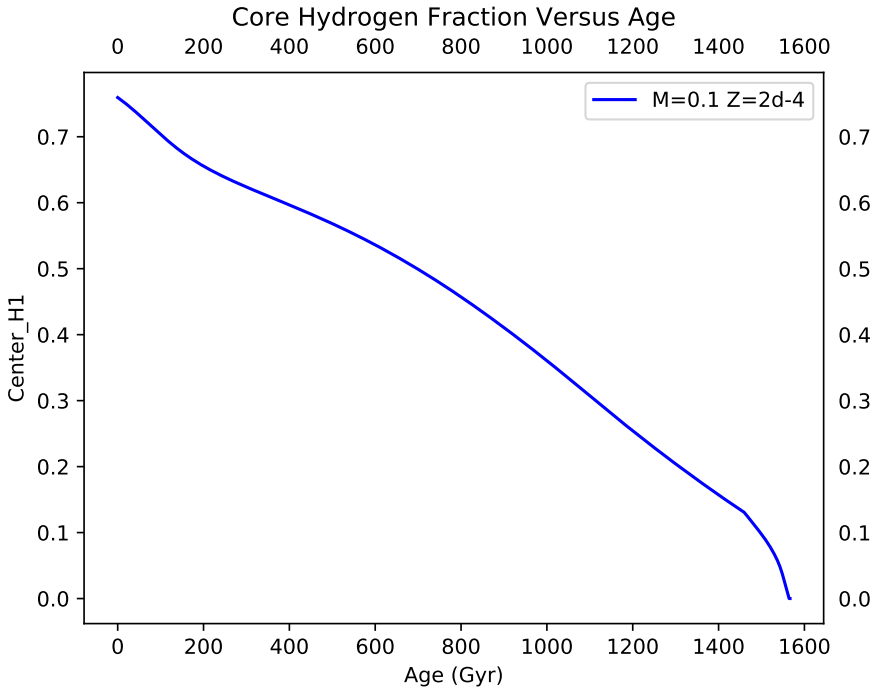

Figure 16. Core hydrogen fraction at 0.1 $M_\odot$ for the model that managed to run.

In the higher mass models which managed to push through the helium flash, another mass-dependent and unique feature is visible. After the helium flash begins, helium shell burning occurs in these models along with hydrogen shell burning. This is interesting, as I had not seen this feature previously as none of my models were able to push past the helium flash. This gives a way to analyze this stage on the AGB. The result is shown in the Kippenhahn diagram below, at 1.1 $M_\odot$, which is plotted versus model number since shell burning only occurs at the end of the model and is not visible if it is plotted versus age.

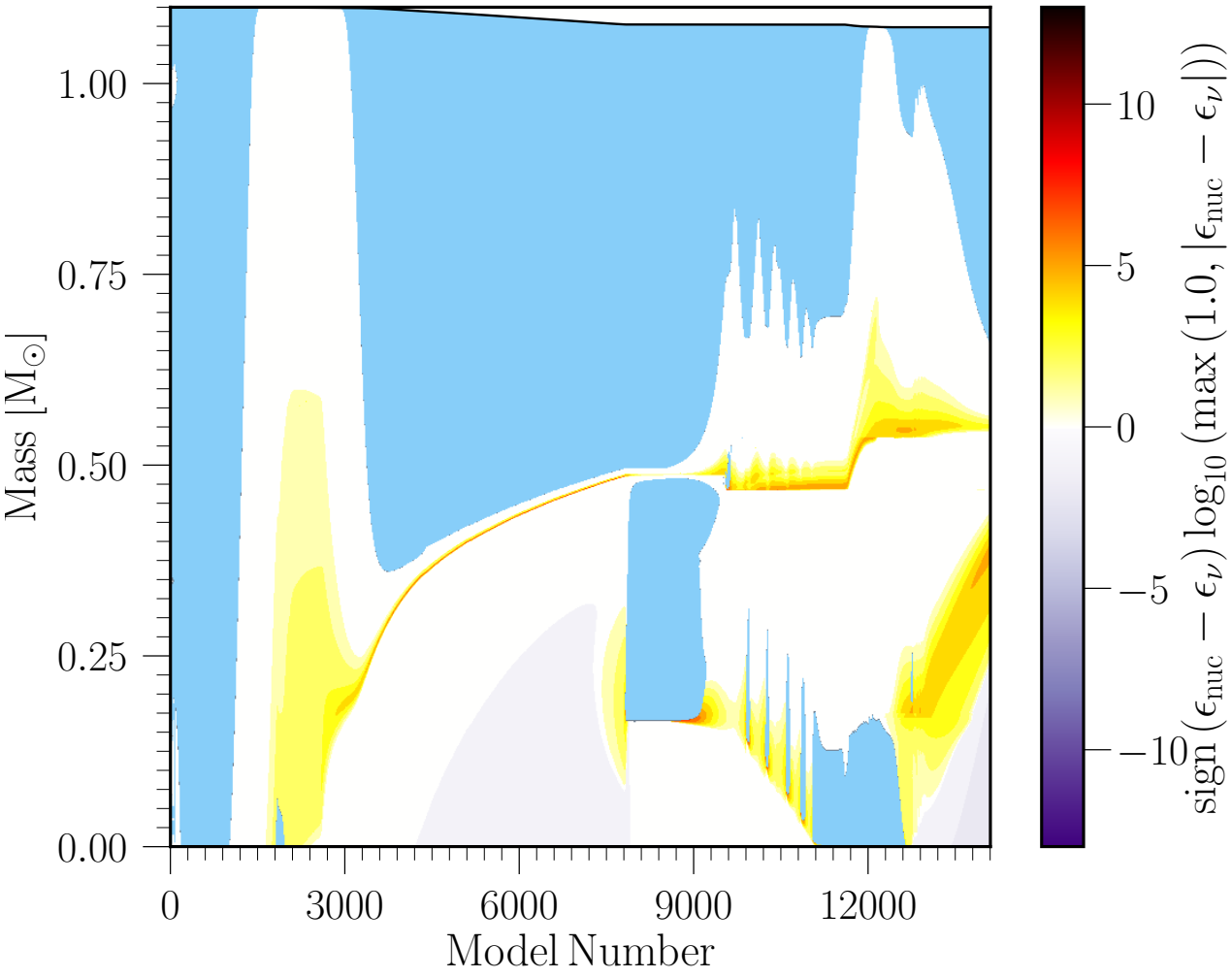

Figure 17. The Kippenhahn diagram for the model at 1.1 $M_\odot$. Past model number 12000, two burning regions, a slightly broader helium burning shell, and a strongly localized hydrogen burning shell, are visible. Energy loss due to neutrino cooling is shown in grey on the opposite side of the heatmap.

In this figure, the helium flash is clearly visible around model number 9000, as burning starts and then moves inwards. It is clear from the diagram that helium burning moves inwards and then as core helium is depleted, helium burning begins as the burning moves back outwards into a shell. Several thermal pulses are visible during the inward helium burning shown as convective episodes in this region.

5. POST-MAIN SEQUENCE EVOLUTION

In another model, these thermal pulses are much more distinct and have an easily observable impact on the HR diagram evolution of the star. For the model at 0.6 $M_\odot$ and Z=10^{-4} $Z_\odot$ post-main sequence evolutionary milestones are clearly visible as this model progressed well past the tip of the red giant branch and onto the AGB. Its HR diagram is shown below, and milestones are marked. This model is chosen since many of the points are distinct.

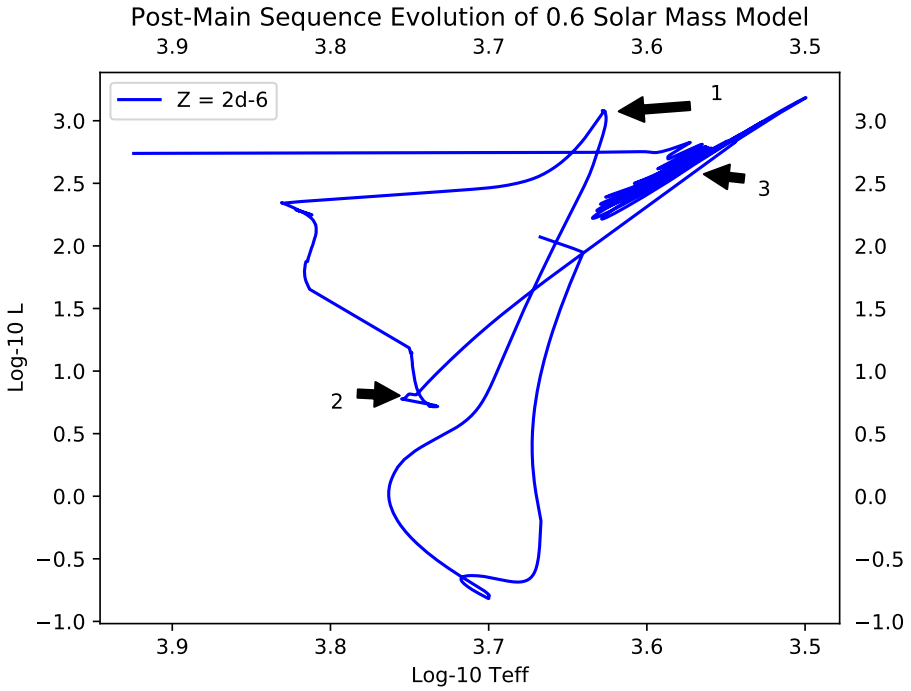

Figure 18. Evolution of a 0.6 $M_\odot$ model with points of interest labeled.

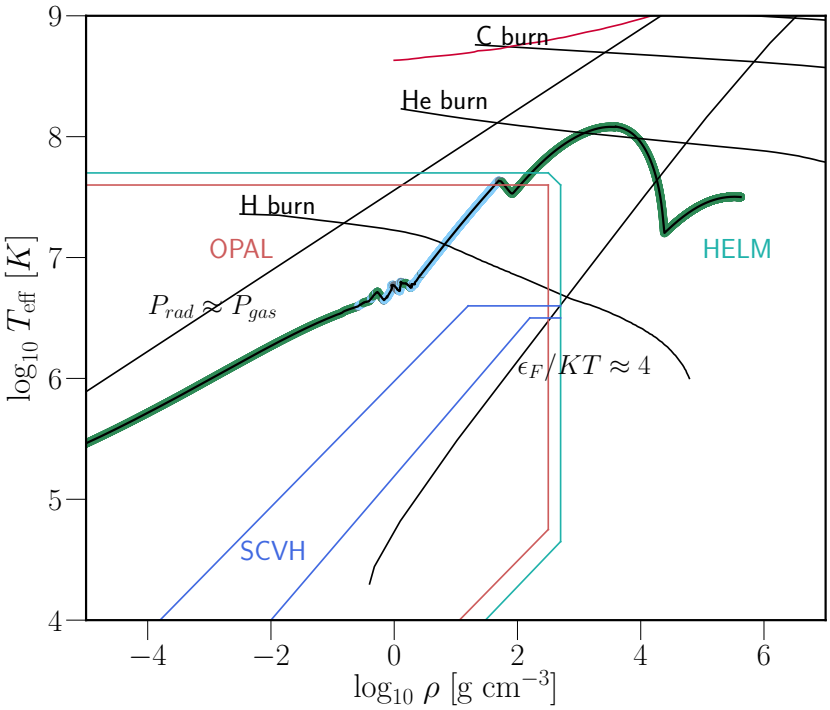

Figure 19. Showing the temperature-density profile of the model in question after timestep convergence. Helium burning has subsided while hydrogen shell burning is producing the vast majority of the energy.

At point 1, where many of the models failed to pass, helium burning has begun and is producing a massive amount of energy at the tip of the red giant branch, though it is not at the core. It begins where the star is hottest, on the hydrogen burning shell which lays on top of a degenerate helium core. This burning lifts the degeneracy and quickly becomes more localized and subsides. This, before, is what I believed to be the only helium burning, as none of my models ever passed this point in their evolution since the timestep between model updates becomes so small that nothing changes.

Given the much longer run time and access to more computing power, the model passed this point. The star is converting a large amount of hydrogen outside the core into helium, with the surface hydrogen fraction dropping by 60 percent, while surface helium fraction increases by nearly the same amount. However the evolution does not stop here. As this is occurring the model moves from the tip of the red giant branch horizontally before it begins to fall in luminosity and reaches point 2.

At point 2, energy generation has decreased by orders of magnitude causing the minimum luminosity observed after the main sequence. The star collapses decreasing in radius and effective temperature while interior temperatures climb as the star moves towards point 3. Once the temperature in the hydrogen burning shell reaches a critical point, the thermal pulses begin occurring, as shown at point 3.

The thermal pulses manifest themselves as the looping behavior shown around point 3 where the star cycles between increasing luminosity and radius and decreasing temperature and decreasing luminosity and radius with increasing temperature. The thermal pulses are caused by buildups of helium left behind by hydrogen shell burning which burn explosively driving the oscillating behavior shown in the HR and temperature-density diagrams.

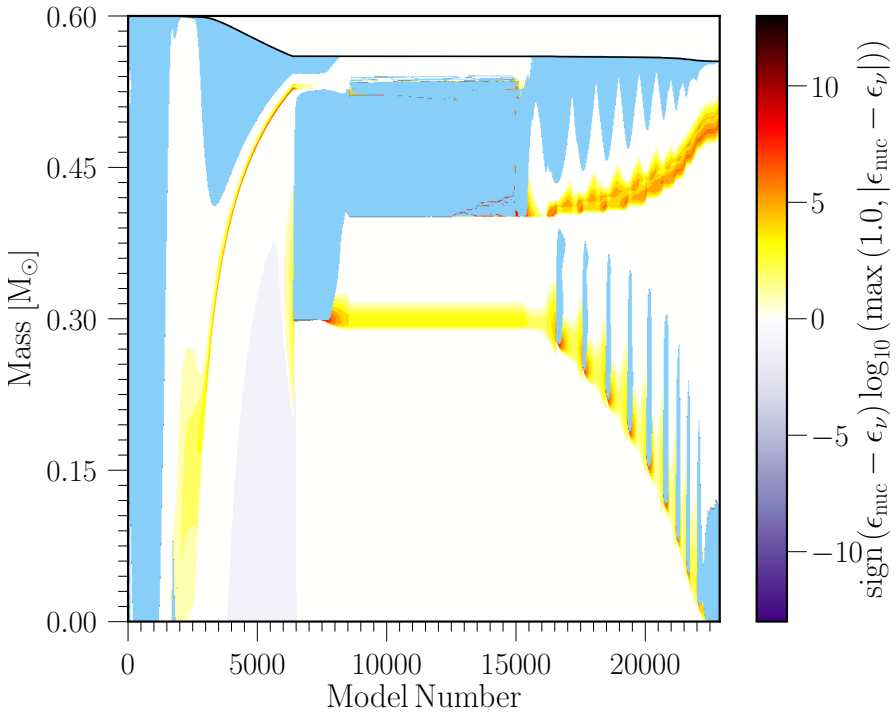

Figure 20. The Kippenhahn diagram for the model in question clearly highlights the thermal pulses moving towards the core.

These pulses move inwards as shells of helium are built and burned, but the burning is so shortly lived that they are unable to produce much carbon. This is shown in the *MESA* live output abundance window, where the helium fraction barely drops by a noticeable amount, on a log scale. The convection caused by these pulses moves inwards and the helium burning is stopped quickly by a drop in temperature. The temperature of the helium shell then begins to increase again as it is able to contract in the absence of significant burning or convection until it reaches the critical point, at which the cycle repeats with the appearance of another explosive shell flash, until this reaches the center of the core.

Another model showcases the last part of post main sequence evolution where the all of the helium in the core is converted to carbon. The star at 0.8 $M_\odot$ and 10^{-4} $Z_\odot$ does this, but its milestones on the HR diagram are not as clearly defined. The Kippenhahn diagram for this model shows burning moving back outwards after a series of thermal pulses.

This model shows the helium core burning, which is what actually creates the carbon-oxygen core. The core temperature at this point exceeds 10^8 K, and consistent helium burning is permitted, which did not happen during the helium flash or thermal pulses. The following temperature-density profile, which looks a lot more like a main sequence model simply reaching a higher temperature and density and thus regularly burning helium, is shown below.

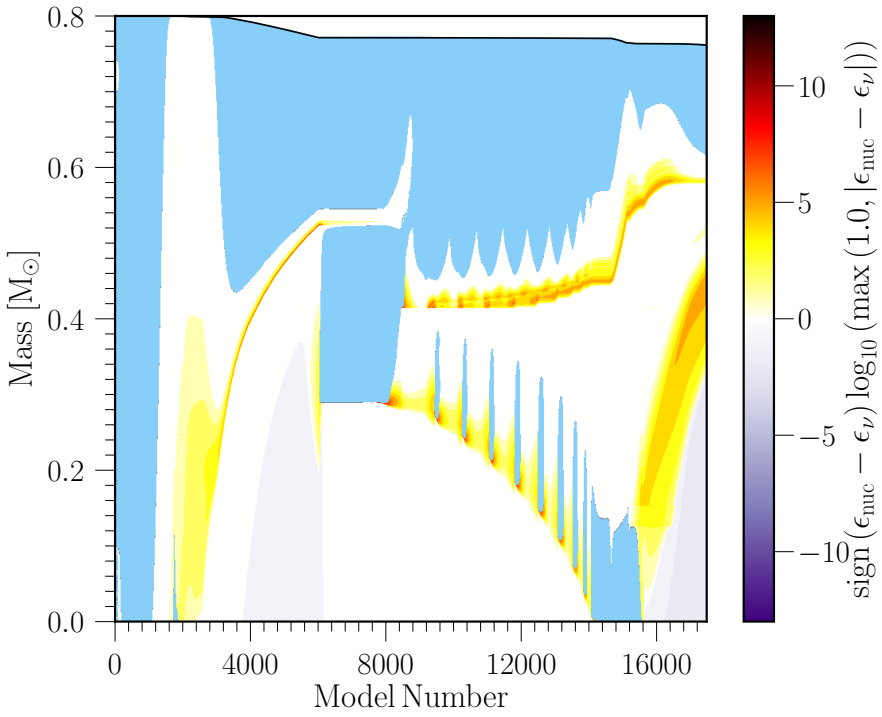

Figure 21. The Kippenhahn diagram going slightly further into post-main sequence evolution, at 0.8 $M_\odot$ and 10^{-4} $Z_\odot$.

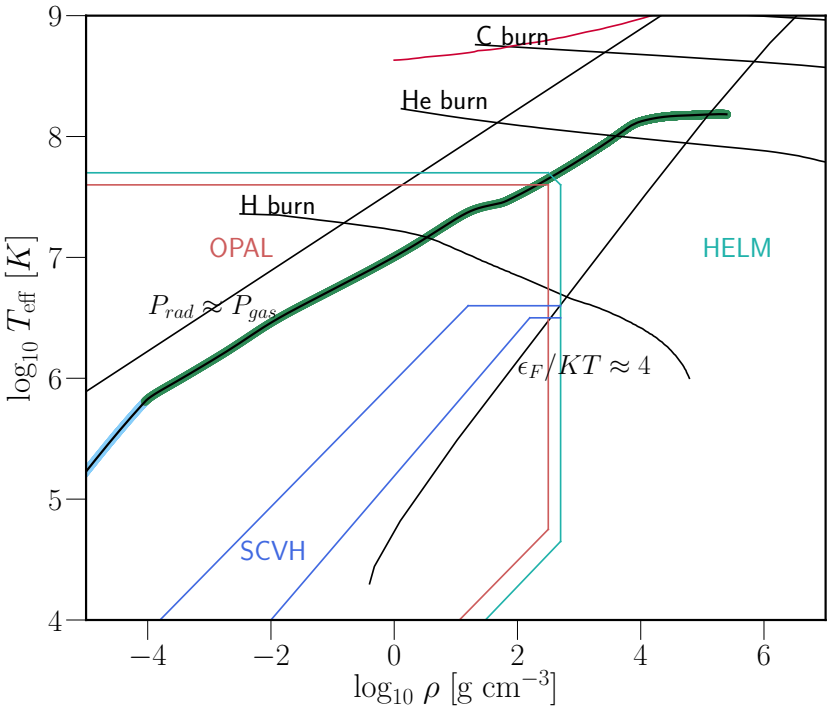

Figure 22. A temperature-density profile taken during core helium burning. A small part of the core, furthest right, has become degenerate and is no longer burning. This is the beginning of white dwarf formation.

This differs from the temperature-density profile taken where a helium white dwarf has begun forming, shown in figure 4. In figure 4, part of the core has already become degenerate but never reached helium burning temperatures, and is thus showing the same qualitative behavior below the threshold for helium burning. Here, the carbon core becomes degenerate as it forms while helium burning moves outwards, and in the helium white dwarf case, a degenerate helium core forms as hydrogen burning moves outwards. One difference seen in the *MESA* output shows that nearly the entire mass of the model in figure 4, 0.488 out of 0.5 $M_\odot$, is left in the core as helium. In the 0.8 $M_\odot$ model making a carbon-oxygen white dwarf, the core only reaches about half of the mass of the star as the model ends, though this may be a result of runtime limitations and not a fundamental difference in how the core evolves.

6. METALLICITY AND STELLAR LIFETIME

In this section, I show the lifetimes of each model as dependent on mass and metallicity. Primarily, I show that there is almost no difference in lifetime until $Z_\odot$ is reached, and when this is not the case, its due to either the model failing to complete due to computing time, or failing to run. In the successful models, solar metallicity stars higher mass have longer lifetimes than models at 10^{-2} $Z_\odot$ at lower masses. Above 0.6 $M_\odot$ the models ran all the way to and in most cases through the helium flash, and thus the final age output was easily taken from the MESA history output. At 0.5 $M_\odot$, however, only some of the models were successful while others went all the way to form helium white dwarfs. Thus for their ages, the value is taken from when the star reaches the tip of the red giant branch before becoming a helium white dwarf.

Mass $M_\odot$	$Z_\odot$	10^{-2} $Z_\odot$	10^{-4} $Z_\odot$	10^{-6} $Z_\odot$	10^{-8} $Z_\odot$	10^{-10} $Z_\odot$	Z=0
0.1	—	1570	—	—	—	—	—
0.2	*893	*638	*595	*539	*602	*572	*542
0.3	*419	*311	*283	*278	*291	*282	*303
0.4	*163	*99.7	*101	*54.9	*102	*75.1	*87.7
0.5	*57.0	71.1	71.1	71.1	*27.4	*37.6	71.1
0.6	84.9	37.5	36.9	37.1	37.1	37.1	37.1
0.7	50.4	21.4	21.0	21.1	21.1	21.1	21.1
0.8	31.1	13.3	13.2	13.1	13.1	13.1	13.1
0.9	20.3	8.78	8.65	8.72	8.72	8.72	8.72
1.0	13.7	6.13	6.14	6.10	6.10	6.10	6.10
1.1	9.55	4.47	4.40	4.45	4.56	4.56	4.53

Table 2. Showing the stellar lifetime in *Gyr* as dependent on mass and metallicity. Elements with no entry were models which failed to run entirely, and entries with asterisks were models which never reached core hydrogen depletion and thus cannot be compared to each other. Never reaching core hydrogen depletion was unique to the mass range between 0.2 and 0.4 $M_\odot$ with some failures at 0.5 $M_\odot$.

Failure to reach core hydrogen depletion was a result of equation-of-state issues where the model sat on the boundary between two different EOS regions. An example of this is shown in the appendix. After a survey of the *MESA* archives, this is not a unique problem to my models.

Metallicity affects on lifetime are a result of two factors. The one easily demonstrated in this paper involves core temperature, since lower Z values increase core temperature and thus increase the rate at which hydrogen is consumed, due to the strong temperature dependence of nuclear fusion rates. The other effect has to do with opacity and how energy is transported through the star. Lower Z values give significantly lower opacities, making it much easier for energy to leave the star, which in turn increases the amount of hydrogen burning needed to support the star. Both of these contribute to higher metallcity stars having lower luminosity, and thus they are able to live for longer on the same amount of nuclear fuel.

7. CONCLUSION

In this work, I set out to find when, if at all, the end stage of stellar evolution as a helium or carbon white dwarf would depend on metallicity. After a previous attempt to reproduce a result in *Windhorst et al. (2018),* in which a solar mass star of zero metallicity never ignited helium, I took a much wider range of masses, attempting to run models from 0.1 to 1.1 $M_\odot$ with varying Z values between zero and $Z_\odot$. I found no case in which metallicity had an effect on final state, and that it only depended on mass. The mass of helium white dwarfs which did manage to form is consistent with what is qualified as a low mass white dwarf which are also believed to be comprised of helium, as stated in *Zenati et al.(2019).*

Despite this, I use the model data to explore a vast amount of mass and metallicity dependent features seen in the data. First, I explain the noticeable yet small difference in core temperatures between $Z_\odot$and *Z=0*, showing that while *Z=0* models have consistently higher core temperatures, that the difference is small, and hence does not create a metallicity dependent division between helium and carbon white dwarf formation.

I then used the data to demonstrate that zero metallicity is a safe approximation for the first stars after being questioned about it when defending previous work. At this mass range which started with big bang relative abundances of around 10^{-10} $Z_\odot$, there is little to no difference in HR diagram evolution. Of those that had differences, the main sequence never ended as core hydrogen was never depleted and finished at different values, making a direct comparison difficult. In the case where they reached the exact same amount of core hydrogen at 0.17, which occurred at 0.2 $M_\odot$, the HR diagram evolution is identical. Finally, even for the highest masses in this survey where heavy elements used in CNO burning serve as catalysts for energy generation, there is no difference between the two evolutionary tracks.

Next, in the absence of new and interesting metallicity dependent features, I show and discuss mass dependent ones. I demonstrate a difference in evolution across the 0.4-0.5 $M_\odot$ boundary in which the core is resupplied with hydrogen for burning as a result of convection. This feature, when explored for all models in the range 0.2-0.4 $M_\odot$, is responsible for the fact that none of these models ever reached core hydrogen depletion or displayed post main sequence evolution. In all of these models, if core hydrogen reached a value just below 20%, then there was a brief episode of convection able to bring hydrogen back into the core, which is displayed in the Kippenhahn diagram at the same ages at which core hydrogen fraction increases, and this is shown for a model where this effect happens multiple times. This never occurs for any mass above 0.4 $M_\odot$ which explains why all of the models except the one that failed were able to reach post main sequence evolution.

I then explore the only 0.1 $M_\odot$ model which managed to run and explain why it did not show this core hydrogen replenishment. I find this model to be continually convective, which is something expected of stars in this mass range. As such, the core is continuously being supplied with hydrogen for burning instead of this happening in discrete episodes. As such, the hydrogen fraction continuously decreases with age, but at a much slower rate even when normalizing to account for age.

I also explore something unique to the higher mass models above 0.5 $M_\odot$. In previous modeling, no model I ran ever made it past the helium flash, but the majority of these models did due to the extra computing time and power. I show post helium flash evolution via a Kippenhahn diagram at 1.1 $M_\odot$. The helium flash occurs and is shown moving inwards while hydrogen shell burning continues, and then reaches the core and begins to move back outwards as helium is depleted. The model shows two burning shells, one of hydrogen and one of helium on the AGB when it was terminated.

In the next section, I explore some of the milestones visible in post main sequence evolution through the HR diagram, explaining its behavior through Kippenhahn diagrams and temperature-density profiles. I highlight the tip of the RGB, which in the past was the final stage reached by any of the models, and then explain briefly why this was the case due to timestep convergence. Then I detail the evolution as the star moves from here to the AGB and thermal pulses, all of which are clearly defined in figure 18.

I then take another model which made it even further and show the effect of helium core burning in figures 21 and 22, and compare the formation of a carbon core to the formation of a helium one, which occurs in figure 4. I find that on a general level, the behavior is the same, where the products of nuclear burning accumulate at the core and become degenerate as the burning moves outwards, forming a degenerate core which will become a white dwarf.

In the final section, I explore one metallicity dependent feature which I did not find previously. In every model which reached the end of the main sequence or further, age is nearly identical for all Z values other than $Z_\odot$. For the select few models at 0.5 $M_\odot$ which actually formed helium white dwarfs, this age is taken from the tip of the red giant branch and no asymptotic giant branch ever occurs. All models above this point reached the AGB by the time they were terminated and showed that metallicity has almost no effect on lifetime unless it is of the order $Z_\odot$. I briefly explain the effect of metallicity on lifetime as a result of opacity and higher core temperature.

After a much more detailed survey of low mass stellar evolution with varying Z values, I am able to make a stronger conclusion about metallicity having no effect on the end stage of stellar evolution. Whether it reaches the AGB and makes a carbon white dwarf, or whether it does not and leaves behind a helium white dwarf seems to only depend on mass, and if ever this will be false, it will be found inside a much finer mass grid between 0.5 and 0.6 $M_\odot$, which was the mass boundary setting apart stars reaching the AGB and those which failed to do so. I am also able to conclude based on ages that no helium white dwarf could yet have formed in the universe from a single star, which I expected to be true.

8. ACKNOWLEDGMENTS

This work was made possible by many different people who contributed both technical and scientific assistance. The research computing team at Arizona State University was critical in obtaining the models and setting up *MESA* on the agave super-computing cluster. The assistance of research computing administrator Gil Speyer was required to complete this project. His help in setting up the environment for MESA to run on the supercomputer made running 77 models a possibility. Graduate student Bhavin Joshi also assisted in retrieving the large amount of data from the supercomputer so that I could analyze it. Finally, my advisers Dr. Rogier Windhorst, Dr. Francis Timmes, and Dr. Patrick Young provided useful scientific feedback which guided me in making correct conclusions about the data. Dr. Timmes also provided the university funding for parts of the computing cluster used to run the models.

Software: `MESA` (Paxton et al. 2011, 2013, 2015, 2018, 2019) `Python` https://www.python.org, `matplotlib` (Hunter 2007), `NumPy` (van der Walt et al. 2011) `MesaPlot` (Farmer, 2020)

REFERENCES

Hunter, J. D. 2007, Computing In Science & Engineering, 9, 90

Paxton, B., Bildsten, L., Dotter, A., et al. 2011, ApJS, 192, 3

Paxton, B., Cantiello, M., Arras, P., et al. 2013, ApJS, 208, 4

Paxton, B., Marchant, P., Schwab, J., et al. 2015, ApJS, 220, 15

Paxton, B., Bauer, E., Schwab, J., et al. 2018, ApJS, 234, 34

Paxton, B., Smolec, R., Schwab, J., et al. 2019, ApJS, 243, 10

Pols, O. R., Tout, C. A., Lattanzio, J. C., Karakas, A. I. 2001. Thermal Pulses and Dredge-up in AGB Stars. Evolution of Binary and Multiple Star Systems 31.

rjfarmer/mesaplot: (Version v1.0.8). https://github.com/rjfarmer/mesaplot/tree/v1.0.8

van der Walt, S., Colbert, S. C., & Varoquaux, G. 2011, Computing in Science Engineering, 13, 22

Vassiliadis, E., Wood, P. R. 1993. Evolution of Low- and Intermediate-Mass Stars to the End of the Asymptotic Giant Branch with Mass Loss. The Astrophysical Journal 413, 641.

Windhorst, R. A., Timmes, F. X., Wyithe, J. S. B., et al. 2018, ApJS, 234, 41

Zenati, Y., Toonen, S., Perets, H. B. 2019. Formation and evolution of hybrid He-CO white dwarfs and their properties. Monthly Notices of the Royal Astronomical Society 482, 1135.

9. APPENDIX

Despite having to omit this model, I still include its HR diagram here to show why it was necessary. The problem occurred during the main sequence, where as seen in the MESA output images, normal PP chain burning was almost immediately replaced by a large spike in energy generation at the core generating in excess of 10^{10} ergs / gr / s. This is obviously not a physical model this did not happen for any of the other models, and does not make any sense. Hence this model is not considered for the purposes of comparing big bang and zero metallicity evolution. This power-law growth in luminosity was seen in a few of the other models at lower masses, but not to such an extreme.

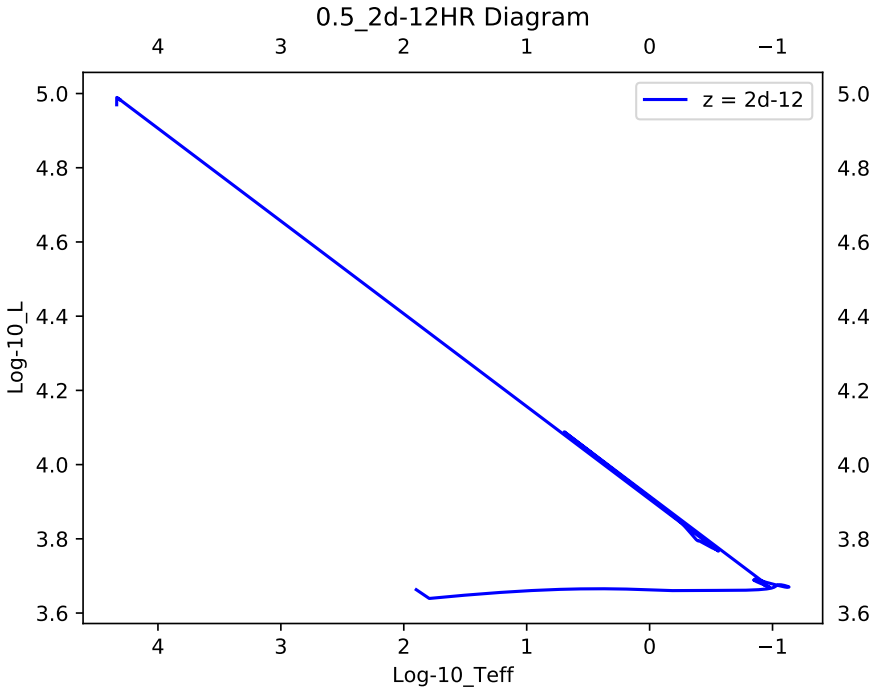

Figure 23. Showing the model at 0.5 $M_\odot$ and 10^{-10} $Z_\odot$ which appears to have a luminosity in excess of 10000 $L_\odot$ for part of its evolution.

This failure occurs in MESA when the model sits on an equation of state boundary, which helps explain why the calculations failed. The temperature-density profile remains in this region for every model which failed for reach hydrogen depletion. After discussing this behavior with one of my advisers, I conclude that while it is not an error, it is a case in which one must be able to interpret the results and not take them as fact.

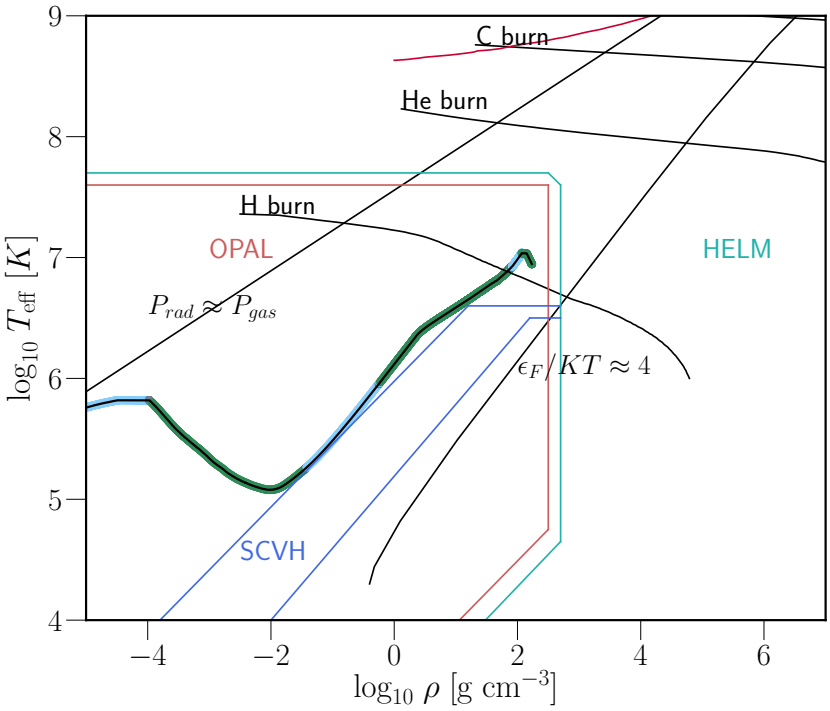

Figure 24. Showing the model at 0.5 $M_\odot$ and 10^{-10} $Z_\odot$ which sits on the equation of state boundary between two regions, which are labeled. The luminosity growth is a result a P-P burning flash generating energies in excess of 10^{10} ergs / gr / s, which should not happen and can be safely dismissed.